Chapter 5. Velocity Estimation

Introduction

In chapter 1 we noted that because most conventional velocity estimation techniques assume horizontal reflectors their performance tends to degrade when the reflectors are curved, dipping or discontinuous. In this chapter we make a more detailed study of this degradation. On the basis of this study, we conclude that velocity estimates may be improved if they are based on downward continued data rather than on surface data. Using two synthetic examples we show both that velocity estimates can be improved by downward continuation and that this improvement does not depend critically on the velocity used in the continuation equation. Next we discuss how downward continuation might be used to allow accurate velocity estimates to be made from data recorded in areas where the reflectors have little lateral continuity. As a finale we illustrate the effects of downward continuation on velocity estimates made from some Gulf Coast field data.

Effects of Reflector Structure on Velocity Estimates

Levin (1971) showed that, when viewed on a common midpoint gather, the arrival times of reflections from dipping planes follow hyperbolic trajectories. Levin also showed that the rms velocities, v_{rms}, obtained from such data are always greater than the true wave velocity $\tilde{v}$. Specifically, the relationship is

$$v_{rms} = \tilde{v}/\cos(\phi) \qquad (5\text{-}1)$$

where ϕ is the dip of the reflector and $\tilde{v}$ is the true velocity.

Figures 5-1 and 5-2 illustrate this dip dependence of velocity which we shall call the Levin effect. Frame 5-1B shows moveout corrected gathers which would be recorded over a point scatterer. Residual moveout

caused by the Levin effect is readily apparent on these data. The velocity estimates which would be made from the data of Figure 5-1 are shown in Figure 5-2. The coherence of each common midpoint gather along the various hyperbolic trajectories $\tau(d_0 , h , v_{rms})$ is displayed on the midpoint versus time plot of Figure 5-2. The hyperbolic trajectories, $\tau(d_0 , h , v_{rms})$ are given by

$$\tau(d_0 , h , v_{rms}) = (d_0^2 + \frac{4h^2}{v_{rms}^2})^{1/2} \qquad \text{where} \qquad (5\text{-}2)$$

d_0 is a zero offset travel time. The coherence measure, $c(y , v_{rms})$, is a partially normalized sum of the data along each trajectory, given by

$$c(y , v_{rms}) = \frac{\sum_{d_1}^{d_2} \left(\sum_{h=0}^{h_{max}} Q(y,\tau) \right)^2}{\left\{ \sum_{d_1}^{d_2} \sum_{h=0}^{h_{max}} (Q(y,\tau))^2 \right\}^{1/2}} \qquad (5\text{-}3)$$

For Figure 5-2 the outer time gate, (d_2-d_1), included all of the data in Figure 5-1. Peak values of $c(y,v_{rms})$ indicate the best estimate of velocity for each midpoint. As predicted by equation (5-1), velocity error is greatest where the apparent dip of the data is largest.

Often equation (5-1) is the only correction needed to obtain true velocities from the rms velocities of reflections from curved or dipping interfaces. To make this correction, dip must be estimated directly from the data. Usually, this is not difficult. Problems arise when there are conflicting dips or when there is rapid horizontal dip variation. Diffracted events are also a problem since their apparent dip as measured on a section is not necessarily the angle needed for equation (5-1). Figure 5-3 illustrates problems which can be encountered with point scatterer diffractions.

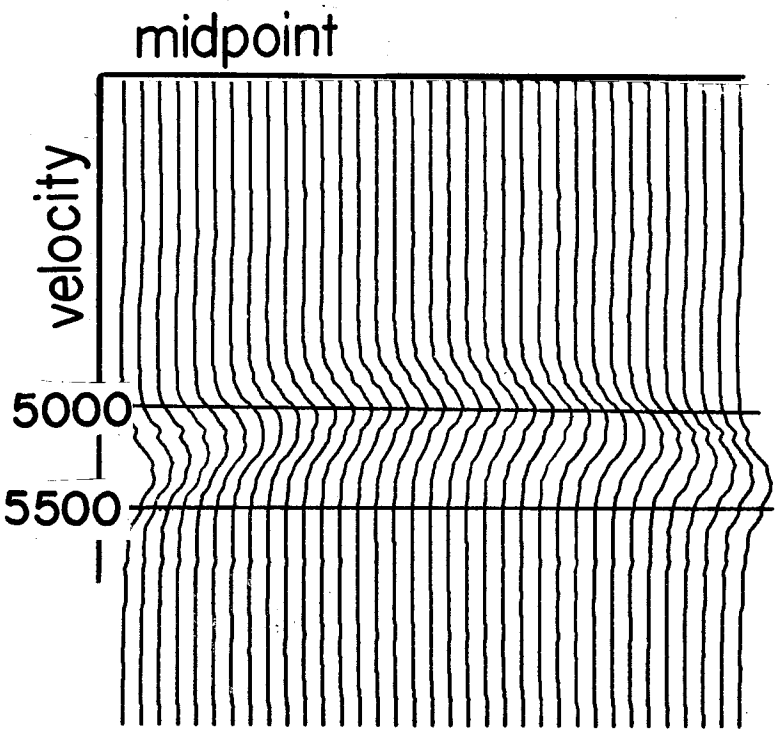

Figure 5-2. Velocity estimates for the data of Figure 5-1. Displayed on the velocity versus midpoint plot, is a partially normalized sum of the CMP gather data along hyperbolic trajectories corresponding to various rms velocities. Peak values indicate the best estimate of velocity for each midpoint. True velocity is 5000 ft/sec. Estimated velocities are highest where the apparent dip of the data is greatest. Velocity estimates are correct near the scatterer where the dip of the data is nearly zero.

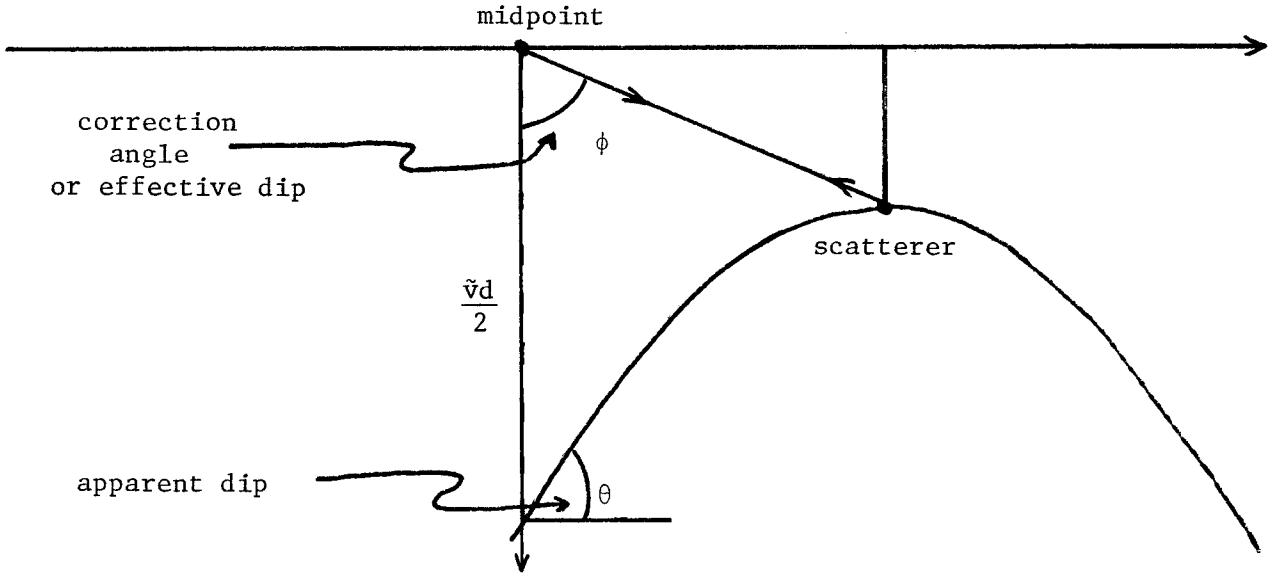

Figure 5-3. Apparent dip of diffraction events cannot be used to correct moveout velocities for the effects of structure. At midpoints far from the scatterer, the apparent dip of the diffraction is independent of shot and receiver location. The dip is governed solely by the asymptote of the hyperbola. For these midpoints the ray paths for all offsets are nearly horizontal. Because of this, the travel times of the reflections are nearly independent of offset and the moveout velocity is very large. As the midpoint goes to infinity, travel time becomes independent of offset and the moveout velocity becomes infinite. In thiscase equation (5-1) requires the correction angle to be 90°. Clearly the apparent dip of the data cannot be 90°, since that would imply that the material velocity was zero. The angle required to correct the moveout velocities is shown in the figure as ϕ. Note that ϕ becomes 90° for midpoints far from the scatterer. Since measurement of ϕ requires knowledge of the scatterer position, we can conclude that dip estimation for diffracted data cannot be a local process.

Reflections from a point scatterer illustrate a second characteristic of non planar data which can cause difficulties for velocity estimators. The hyperbolic arrival times of point scatterer reflections tend to diffuse velocity information away from the scatterer location. Even if accurate dip corrections are made, erroneous velocity estimates may be obtained from these data because the location of the estimate may not coincide with the reflection point of the waves upon which the estimate is based. Scatterer data illustrates the general principle that reflections from non-horizontal reflectors, tend to diffuse velocity information in both space and time. Since the dip angles encountered in reflection seismology are generally less than 45°, velocity information tends to diffuse more horizontally than vertically. Thus, diffusion is most important when velocity is laterally variable. However, even in the laterally invariant velocity models treated in this thesis, velocity diffusion may result in contamination of deep velocity estimates with estimates based on reflections from shallow non-horizontal reflectors.

Preprocessing with Downward Continuation

The incorrect positioning of velocity estimates which we have called velocity diffusion occurs when the location of a portion of data on a seismic section does not coincide with the location of its reflection point. In earlier chapters we found that downward continuation can be used to position or migrate all data on a section to their reflection points. We can exploit this property of downward continuation to improve velocity estimates by using downward continuation as a preprocessor for conventional velocity estimation techniques. If we do this, the resultant velocity estimates should not exhibit any velocity diffusion effects.

This approach has an additional advantage: it suppresses errors due to residual moveout caused by the Levin effect. To see why this occurs, consider data recorded over a point scatterer. Velocity estimates made from such surface data must be dip corrected as indicated in equation (5-1) and Figure 5-3. Migration collapses point scatterer hyperbolics to focuses for which dips measured as shown in Figure 5-3 are zero. Because of this, equation (5-1) implies that no dip corrections are necessary for velocity estimates based on downward continued scatterer data. Since the wave equation is linear, we can conclude that no dip corrections are necessary for any reflector geometry, on the basis of this point scatterer example.

Figures 5-4 through 5-7 demonstrate the usefulness of downward continuation in removing diffusion and Levin effect phenomena from velocity estimates. Figure 5-4 shows the earth model used to generate the data for 5-5, 5-6 and 5-7. The leftmost frames of 5-5 show two moveout corrected common offset sections generated by using the data of 5-4 as initial conditions in the time reversed version of equation (4-23). Differences between the near trace section and the far trace section are due to structurally caused residual moveout. The center frames of 5-5 show the same surface data after migration. The rightmost frames show the data after migration with 10% too low of velocity. In spite of the erroneous velocity, migration has removed most diffraction effects from these data.

Figure 5-6 shows moveout corrected gathers constructed from the data of Figure 5-5. The surface gathers exhibit much structurally caused residual moveout. The migrated gathers, on the other hand, are independent of offset. The undermigrated gathers on the far right of Figure 5-6

Figure 5-5 cont'd.

frames are moveout corrected surface data sections constructed by using the earth model of 5-4 as initial conditions in the time reversed version of equation (4-23). Water velocity was used for both the moveout and migration velocity. The upper frames are small offset data (h=600') . The lower frames are large offset data (h=3600'). The center frames show the surface data after migration. Reconstruction is not exact due to dip filtering used in generating the surface data. The rightmost frames show the same surface data after migration with a velocity which was 10% too small. In spite of the incorrect velocity, most of the diffractions apparent in the surface data have been removed by downward continuation. These frames illustrate the fact that migration quality is moderately insensitive to velocity error if reflector dips are not large.

illustrate that downward continuation, even with an erroneous velocity, can result in dramatic reductions in velocity diffusion and Levin effect phenomena.

Figure 5-7 depicts the velocity estimates made from two common midpoint gathers of the data of Figure 5-5. The locations of the gathers are given by the arrows in Figure 5-4. Velocity estimates based on surface data are shown on the left of 5-7. Estimates based on migrated data are shown on the right. Velocity diffusion causes the number of 'events' on the surface estimates to be larger than the number on the migrated estimates. Erroneous velocity estimates caused by the Levin effect are apparent on the surface estimates.

The migrated data for Figures 5-4 through 5-7 were constructed with equation (4-23). Thus, each common offset section was migrated separately, using a constant moveout and continuation velocity. The moveout and continuation velocities were the same as that used to generate the surface initial conditions. Because of this, these figures demonstrate only that downward continuation with the true velocity allows accurate estimation of that already known velocity.

Downward Continuation with Erroneous Velocities

When downward continuation is used in a velocity estimation scheme, the choice of a continuation velocity must be made before the true velocities are determined. This order of operations almost guarantees that the continuation velocities used in velocity estimation will differ from the true velocities. In the preveous section we demonstrated that continuation with the correct velocity, results in improved estimates. Here we attempt to analyze the results which can be expected in the realistic case where the continuation velocity is incorrect.

To do this we need to consider equation (4-9) from the previous chapter. Copying this equation from chapter 4 we have

$$Q_{dr} + \frac{h}{d}(\partial_y + \partial_h) Q_r = -\frac{v\alpha^2}{2\beta^2}\left(\frac{d^2}{4} + \frac{r^2h^2\gamma}{v^4d^2}\right)(\partial_y + \partial_h)^2 Q$$

$$+ \frac{hr\alpha^2\gamma}{v^2 d\,\beta}(\partial_y + \partial_h)Q_d - \frac{\alpha^2}{2v}\gamma\, Q_{dd} \qquad (5\text{-}4)$$

where

$$\alpha^2 = 1 + \frac{4h^2}{v^2d^2} \;;\; \beta = d - r/v \text{ and } \gamma = \left(1 - \frac{v^2}{\tilde{v}^2}\right) . \qquad (5\text{-}5)$$

Equation (5-4) is a continuation equation which is valid for a constant moveout velocity, v, but a variable wave velocity $\tilde{v}$. The γ dependent terms of (5-4) turn on only when the moveout correction velocity differs from the true velocity. Thus, one way of analyzing the errors that may result from continuation with an erroneous velocity, is to examine the γ dependent terms of equation (5-4) We shall use that approach here. In analyzing (5-4) we will neglect the effects of amplitude variation due to geometrical spreading and of wavelet stretching due to moveout correction. In making the analysis, we will examine each type of term in (5-4) in succession. If a term is found to be unimportant under some reasonable assumption, we will drop it from the continuation equation. After making all reasonable deletions, we will compare the resulting equation to (4-23), the equation used earlier to remove structural effects when velocity was known. If these two equations are markedly different we can expect some problems to result from downward continuation with (4-23).

As a first step in the analysis we will drop the Q_{hr}, Q_{yr} and Q_{yh} terms on the basis of the arguments given in chapter 4. Next

we study the behavior of the remaining terms of (5-4) under the assumption that the earth's velocity structure is layered and that the reflectors have no dip. In this case $Q_y = 0$ and terms depending on Q_y may be dropped from (5-4) leaving

$$Q_{dr} = -\frac{v\alpha^2}{2\beta^2}\left(\frac{d^2}{4}+\frac{r^2h^2\gamma}{v^4d^2}\right)Q_{hh}+\frac{hr\alpha^2\gamma}{v^2d\beta}Q_{hd} - \frac{\gamma}{2v}\left(1+4h^2/v^2d^2\right)Q_{dd} \tag{5-6}$$

Although equation (5-6) looks complicated what it does is not complicated. If $\gamma=0$, the design of the coordinate system requires that surface and buried receiver data be equivalent. Thus, when $v=\tilde{v}$ and $Q_y=0$ continuation with (5-6) is a null operation. When $\gamma\neq0$ the situation is a bit different.

Moveout correction of surface data requires correction for both the upgoing and downgoing legs of the reflection path. Buried receiver data requires correction only for the downgoing path. Residual moveout caused by differences between the true velocity and the moveout correction velocity is associated with both legs of a reflection path. Therefore, when $\gamma\neq0$ buried receiver data have half the residual moveout of surface receiver data (here we are considering the travel times of the zero offset arrival to be part of the residual moveout). In the case we are studying, this reduced moveout is the main difference between surface and buried receiver data. Accordingly, when there is no dip and $\gamma\neq0$, the main result of continuation with (5-6) is a 50% reduction of residual moveout.

If the residual moveout of an event is small compared to its zero offset travel time, one can show that the time shifting term of equation (5-6), Q_{dd}, performs virtually all of the required moveout reduction. Thus, when velocity error and offset are moderate, the terms depending on Q_{hh} and Q_h in (5-6) do not significantly affect the downward continued data and they may be neglected. If downward continuation is used as part of a velocity estimation procedure it may not be desirable to model behavior governed by any of the h dependent terms of (5-6), including Q_{dd}. This is because there is a great practical advantage to be gained by insuring that residual moveout due to non-zero values of γ be independent of receiver depth. If this is done, most velocity estimation programs designed for use on surface data can be applied to downward continued data without modification. It is for this reason that in velocity estimation applications we will drop all the h dependent terms in (5-6), giving a continuation equation of the form

$$Q_{dr} = -\frac{v}{2}\frac{\alpha^2}{\beta^2}\left(\frac{d^2}{4}+\frac{r^2h^2\gamma}{v^4d^2}\right)Q_{yy}+\frac{hr\alpha^2\gamma}{v^2d\,\beta}Q_{dy}-\frac{\gamma}{2v}Q_{dd} \qquad (5\text{-}7)$$

By choosing to ignore the h dependent terms of (5-6) we have lost the ability to accurately model situations where velocity varies horizontally. More precisely, we have made the assumption that velocity does not vary significantly over distances comparable to the receiver cable length. Since this is the assumption made when velocity is estimated on the basis of correlations of data along hyperbolic paths, we feel that it is justified here. This assumption along with the fact that our continuation equations do not downward continue sources, is the main reason that the methods given in this thesis are strictly valid only for the first class earth models discussed in chapter 1.

The final term in (5-7) we shall consider is the Q_{dy} term. As we noted above, when $\gamma \neq 0$ correctly downward continued data have residual moveout, including an incorrect zero offset travel time. A look at the definition of y in equation (4-1b) shows that y depends not only on the source and receiver coordinates, (g,s,z), but also on v and t. This dependence along with the residual moveout causes each offset of the correctly migrated data corresponding to the same reflection point to appear at a different position on the y axis. This effect is undesirable because it means that migrated common midpoint gathers are not common reflection point gathers. Integration over d using a high frequency assumption shows that Q_{dy} is a horizontal shifting term. Its predominate function is to shift, without change of form, each offset of the data a different distance along the y axis. Because of this, we conclude that Q_{dy} models the undesirable effect discussed above. Since we don't need to model this effect we will delete the Q_{dy} term from (5-7) leaving

$$Q_{dr} = -\frac{v\alpha^2}{2\beta^2}\left(\frac{d^2}{4} + \frac{r^2h^2\gamma}{v^4d^2}\right) Q_{yy} - \frac{2\gamma}{v} Q_{dd} \qquad (5\text{-}8)$$

Notice that we could have used this same reasoning to delete the other horizontal shift term, Q_{hd}, had it not been neglected earlier.

Equation (5-8) is the equation we will compare to (4-23) to get an idea of how large migration velocity error must be before downward continuation causes degradation of velocity estimates. Copying equation (4-23) from chapter 4 we have

$$Q_{dr} = -\frac{v}{8}\left(\frac{d}{d-r/v}\right)^2\left(1 + 4h^2/v^2d^2\right) Q_{yy} \qquad (5\text{-}9)$$

If γ is such that (5-8) differs markedly from (5-9) we should expect some problems to develop with the downward continuation.

Consider first, the coefficient of Q_{yy} in (5-8). Substituting for α^2 and β^2 and rearranging we have

$$-\frac{v}{2}\frac{\alpha^2}{\beta^2}\left(\frac{d^2}{4}+\frac{r^2h^2\gamma}{v^4d^2}\right) = -\frac{v}{8}\left(1+\frac{4h^2}{v^2d^2}\right)\left(\frac{d}{d-r/v}\right)^2\left(1+\overline{\frac{4r^2h^2\gamma}{v^4d^4}}\right) \quad (5\text{-}10)$$

The over-barred term in equation (5-10)represents a difference between (5-8) and (5-9). For reasonable values of h and γ this term is small and its absence from (5-9) will not cause much error. For $v = 1.2\,\tilde{v}$ and $45°$ emergence angle (θ in Figure 4-1) its average value is .03 .

Next consider the time shifting term Q_{dd} . Since it shifts all offsets equally, the lack of this term in (5-9) cannot, by itself, degrade velocity estimates. However, since the coefficient of Q_{yy} depends on d , the time shifting done by Q_{dd} indirectly changes the value of this coefficient. Fortunately, the effects of this change are small because the time shifting does not change the average value of the Q_{yy} coefficient. A more important effect results from the fact that migration requires data to be downward continued until $r=\frac{vd}{2}$ (until the receivers are at the estimated reflector depth). The Q_{dd} term changes the depth of each portion of the data such that it will be nearly correctly migrated using equation (5-8) when $r = \frac{\tilde{v}d}{2}$. Thus, if $v > \tilde{v}$, the Q_{dd} term shifts data to earlier arrival times. This means that the lack of Q_{dd} in (5-9) will cause the data to be overmigrated (the receivers will be continued past the reflectors) when $v > \tilde{v}$. This overmigration will result in an incomplete removal of velocity diffusion

and Levin effect phonomena from the downward continued data. However, since continuation with (5-9) will partially remove these effects from the data, velocity estimates based on data continued with (5-9) should be more accurate than those based on surface data.

In summary we can conclude that the use of an incorrect downward continuation velocity will result in an incomplete removal of velocity diffusion and structurally caused moveout. For data fitting our earlier assumptions and for moderate velocity errors, the amount of structurally caused moveout remaining after migration is approximately linearly related to the degree of data over or under migration. Thus, for a continuation velocity error of 10%, approximately 10% of the surface structural moveout remains after downward continuation.

Additionally, we can conclude that, if the continuation velocity error is such that the data are not grossly over migrated (by a factor of 2 or more) velocity estimates cannot be degraded by preprocessing with downward continuation. Thus, for reasonable velocity errors downward continuation should always make some improvement in velocity estimates. In cases where the initial migration velocity is quite a bit in error, more than one iteration of migration may be necessary to obtain accurate velocity estimates.

Figures 5-8, 5-9 and parts of Figures 5-5 and 5-6 depict calculations which illustrate these results for velocity errors of 10%. The success of the migration preprocessing on the point scatterer events of Figures 5-8 and 5-9 is especially important because the linearity of the wave equation guarantees that the same quality results will be obtained for all reflector geometries.

Figure 5-8 Cont'd.

Moveout velocity was 5500 ft/sec. The two hyperbolas were constructed with two different velocities (top is 5000 ft/sec, bottom is 5500 ft/sec). Since we are not simulating a variable velocity medium, these initial conditions should be thought of as two separate models that have been displayed on the same grid. Trace spacing is 31 ft. Time ranges from 1.52 to 2.42 seconds. The left frame is a zero offset section. The right frame is a large offset section (h=4000'). Notice that the arrival time of the apex of the deep hyperbola is independent of offset. This occurs because the true velocity of this event equals the moveout velocity. Residual moveout causes the upper hyperbola to appear late on the large offset sections.

The bottom frames show the sections after migration with the equation

$$Q_{dr} + \frac{h}{d} Q_{yr} = - \frac{v}{8} \left(1 + \frac{4h^2}{v^2}\right) \left(\frac{d}{d-r/v}\right)^2 Q_{yy}$$

Migration has collapsed the hyperbolas to focuses on both sections. Because the migration velocity was 10% too high for the shallow hyperbola, we should expect it to be over-migrated. The focus does have some upward curvature but the effect is small. Migration quality is not very sensitive to velocity error.

Velocity Estimation in the Absence of Structural Continuity

Despite its overall success as a geophysical exploration tool, the reflection seismic method is, in some locations on earth, of little use in determining the structure of the subsurface. In these regions seismic data sections are characterized by having very little lateral coherence. Such regions are usually called no-record-areas.

It is often thought that minimal amounts of useful information about the earth can be extracted from data recorded in no record areas. In locations where the lack of data coherency is the result of poor depth penetration caused by near surface attenuation or scattering, this conclusion is probably correct. However, in areas where the poor data coherence is the result of the small coherence length of the earth itself, the use of downward continuation may make it possible to extract usable velocity information from no record data in spite of their randomness. Two geological regions which could possibly result in this latter type of no record data are heavily faulted regions and the interior regions of salt , shale or igneous intrusions.

One model of the latter type of no record area is an earth consisting of a random distribution of point scatterers. The data that would be recorded over such a model are a random function of both midpoint and time and thus appear as no-record data. Interference of events generated by scatterers located at adjacent midpoints coupled with the Levin effect may also make such data fairly complicated functions of offset. Conceivably, for some earth models the effects of interference may be large enough to cause serious degradation of velocity estimates made from surface data recorded over those earth models. In a noise free constant velocity environment this degradation might be manifested

as estimates which are either incorrect or spatially variable. Since interference reduces the total coherence of the data along the best fit hyperbola of velocity estimators, degradation might also take the form of a marked susceptibility of velocity estimates to external noise sources in a noisy environment.

By now it should be apparent that many of the difficulties associated with interference in random earth no record data can be avoided if the data are migrated before velocity estimates are made. Using this approach one can remove much of the Levin effect and interference phenomena from the data. An additional advantage of using migration is that it can accommodate the effects of reflector geometry even when the reflectors are random in three dimensions. In the three dimensional case it is necessary to regard z as a radial distance from the line of the section rather than a depth.

Figures 5-10 and 5-11 show results which illustrate the properties of both surface and downward continued random point scatterer data. Figure 5-10 shows an earth model and the surface data which would be recorded over that earth model. The earth model simulates a random distribution of point scatterers which increases in density from right to left on the frame. The model was created by convolving, in time, a wavelet over a set of random numbers. The resultant data were then smoothed over midpoint with a (1, 4, 6, 4, 1) filter. Smoothing was required to meet the gridding and dip restrictions of the migration equations which were subsequently applied to these data.

Frame B of Figure 5-10 shows the surface data that would be recorded over the earth model. Dip filtering and the finite scatterer size have concentrated most of the energy in Frame B in the portion of each point scatterer hyperbolic which is near the point scatterer. Thus, in spite

Fig. 5-10 Cont'd.

limited the maximum dip in Frame B to about 20°. Such steep dips are visible on the right of the frame where the scatterer density is low. Since the earth model and the surface data appear equally random on the left of the frames, migration can be expected to produce little enhancement of midpoint coherence for these data.

of the approximately 20° dips shown on the right of the frame, most of the energy in Frame B is concentrated in low effective dip events (measured as shown in Figure 5-3).

Figure 5-11 depicts the surface and downward continued gathers constructed from the data of Figure 5-10. Residual moveout is apparent on the surface gathers especially toward the right of the frame. Residual moveout is smaller on the left where both interference and the scatterer density are large. Like residual moveout, offset coherence also decreases toward the left side of the surface data frame. Unlike the surface data, the downward continued data show no residual moveout and excellent coherence in offset.

The absence of interference and residual moveout in Frame B of Figure 5-11 indicates that velocity estimates based on the data of that frame should be superior to those based on the Frame A data. Extending these results to field data and to the earth itself, we can conclude in principle at least, that migration should allow accurate velocity estimates to be made from no record data recorded over reflectors which have little or no continuity.

Interference in Random Scatterer Data

In the previous section we discussed how migration could be used to improve velocity estimates made from random earth data and from some types of no record data. The synthetic example of Figures 5-10 and 5-11 illustrated the magnitude of improvement that could be expected for a particular earth model. Because of the small residual moveout and the high offset coherence of the surface data of Figure 5-11 an unbiased reader may question whether the improvement indicated in 5-11 is worth the cost of performing the downward continuation. To both answer this question and to gain some perspective on the effects of downward continuation in

random scatterer earth models we shall need to study in detail the interference which occurs in the surface data recorded over these models.

To a large extent the importance of this interference depends on the predominant wavelength, λ , of the energy used to probe the point scatterer earth models. Even though an earth model may be random from point to point, any reconstruction of that earth model based on surface recorded reflection data must be continuous over distances comparable to the mean wavelength of the surface data. Because of this, in analyzing interference we will consider the earth to be made up of independent regions which are approximately a half wavelength square (half because we use two-way travel times). We shall call these regions pixels. (The term pixel has its origin in the field of satellite imagery where it is used to denote the smallest region resolvable on an image.)

If an earth model is not totally random we must define pixels to be larger than $\frac{\lambda}{2}$ on a side if they are to represent independent portions of that earth model. If these larger pixels are not square then directivity patterns determined by the orientation of the long axis of the pixels must be assigned to each pixel. Non-square pixels might occur if the earth were more random in the vertical direction than in the horizontal direction. Generally, because of the gridding and dip restrictions of our continuation equations, the earth models used in this thesis have pixels which are about twice as long horizontally as vertically.

Figure 5-12 is the main tool we will use in studying interference in random scatterer earth models. For discussion's sake we will be interested only in the portions of the random scatterer earth model which can contribute to the surface data recorded at midpoint y_0 and moveout corrected travel time d_0 . Curve #1 of Figure 5-12 (the circle) shows the locations in the earth model which can contribute to the arrival

at (y_0, d_0) on a zero offset section recorded over the earth model. Curve #2 (the ellipse) shows similar locations for the data arriving at (y_0, d_0) on a moveout corrected large offset section ($h = \frac{vd_0}{2} = z_0$) . Data recorded at offsets smaller than $h = z_0$ will have contributions from points located along ellipses falling between curves #1 and #2.

The arrival seen at (y_0, d_0) on a surface recorded zero offset section can be generated from the earth model by summing the events in the model which fall along curve #1. Thus, much of the energy seen at (y_0, d_0) on a surface recorded section, is the result of the interference of events due to scatterers located outside the pixel centered at (y_0, z_0). One measure of the importance of interference in a portion of data is the ratio of the energy E_i , at (y_0, d_0) , due to scatterers located inside the (y_0, z_0) pixel, to the energy E_e , at (y_0, d_0) , due to scatterers located exterior to this pixel. Since events due to the external pixels tend to destructively interfere we have

$$E_e = N \cdot P \tag{5-11}$$

where P is the mean power in a pixel and N is the number of pixels which can contribute to the data at (y_0, d_0). N can be estimated by dividing the length of curve 1 by the length of a pixel.

Estimating N and using (5-11) we can get an interference measure I , given by

$$I = E_e/E_i = \frac{NP}{P} = \frac{2z_0\phi}{\lambda} \tag{5-12}$$

where ϕ is a polar angle measured as shown in Figure 5-12.

Equation (5-12) is strictly valid only for zero offset data. However if offset is reasonable equation (5-12) will be fairly accurate for non-zero offset data also.

Since most reflection seismic data are such that z_0/λ is in the range of 10 to 100, equation (5-12) indicates that interference is quite large in point scatterer random earth data, even if the maximum values of ϕ in the data are small. Figure 5-13 indicates how ϕ_{max} might be defined for a particular set of data. The interference possible when $\phi_{max} \approx 10°$ is illustrated by the differences between the earth model and the surface data of Figure 5-10.

The offset to offset coherence of surface recorded random earth data may be high even though many interfering events are present in those data. The critical factor which governs coherence in offset is not how many pixels interfere but which pixels interfere to form the data seen at (y_0, d_0). If the data are such that the same pixels interfere on data of all offsets, then coherence in offset will be high. This would be the case if the data were such that interference occurred only between pixels located in regions where ϕ was small (eg. the A region in Figure (5-12). Since the dip filtering and finite scatterer sizes used in generating the surface data for Figure 5-10 have limited ϕ_{max} to approximately 10° , we should expect those data to have much coherence in offset in spite of the large amount of interference known to be present in them. A look at Figure 5-11 shows that the data fulfill this expectation.

Consider data of a form such that the energy arriving at (y_0, d_0) is solely due to point scatterers located in the B region of Figure 5-12. Since the length of arc on curve#1 is smaller for region B than it is for region A, data recorded in this second case will contain

less interference than the A region data considered earlier. In spite of this, the B region data will be much less coherent in offset than the A region data. This occurs because different offsets of the B region data are the result of the interference of markedly different sets of pixels. Correlation between adjacent offsets of B region data can be expected only when the number of offsets recorded is greater than the number of pixel lengths which can be measured along a radial line intersecting curves #1 and #2 (eg., a line like r, s shown at the edge of the B region).

Because the various offsets of data generated by region B scatterers can be expected to be uncorrelated, velocity estimates based on these data will probably be random enough to be of little value. In fact any velocity estimate can be expected to be poor as a result of poor offset coherence if it is based solely on data due to scatterers located in regions where the radial separation between the ellipses corresponding to the smallest and largest offsets used in the estimate is greater than a pixel length. In terms of Figure 5-12 we are saying that estimates based solely on scatterers outside region A will be poor.

In general then, we can consider any energy to be undesirable for velocity estimation purposes if it is the result of scattering from locations external to the region where the radial separation of the large and small offset ellipses is smaller than a pixel dimension. If we assume that the data generated by scatterers interior to this region are independent of offset we can make some simple estimates of the offset coherence of surface recorded random scatterer data. As a coherence measure we will use an energy normalized sum over offset called semblance. The semblance of properly moveout corrected data

along the true velocity trajectory in offset (arrival times independent of h) can be defined as

$$\text{Semblance} = \frac{(\Sigma_h Q(h,d_0))^2}{M \Sigma_h (Q(h,d_0)^2)} \tag{5-13}$$

where M is the number of offsets used in the sum and d_0 is the zero offset travel time at which semblance is measured.

In estimating the coherence of the random scatterer data we shall express equation (5-13) in terms of quantities which are measurable from Figure 5-12. We define these quantities as follows: S is the number of pixels having an intersection with region A; n is the total number of pixels between curves #1 and #2 which are external to region A; and J is the average number of pixels along lines like r-s in regions external to A. J enters into the calculation because some pixels external to A will be summed more than once if there are more offsets than pixels along lines like r-s. Using these definitions we can say that on average, S pixels from region A and $\frac{n}{J}$ pixels from locations external to region A contribute to each offset of the surface data seen at (y_0,d_0). Thus, we can express Q as

$$Q(h,d_0) = \sum_{i=1}^{S} \xi_{ih} + \sum_{k=1}^{n/J} \mu_{kh} \tag{5-14}$$

where ξ is a random variable describing the amplitude of the wave field in the A region pixels and μ is a random variable describing amplitude in the pixels external to A. We will assume that ξ and μ have zero mean and unit variance. Since we have assumed that data generated by region A are independent of offset, ξ is a constant function of h. Since μ deals with pixels external to region A, it has only J degrees of freedom in offset.

To estimate semblance one need only to substitute equation (5-14) into (5-13). We will calculate the numerator first. Performing this substitution the numerator of (5-13), NUM , is given by

$$NUM = \left(\sum_{h=1}^{M} \left(\sum_{i=1}^{S} \xi_{ih} + \sum_{k=1}^{n/J} \mu_{kh} \right) \right)^2 \qquad (5\text{-}15)$$

After doing the inner sums (5-15) becomes

$$NUM = \left(\sum_{h=1}^{M} \left(\sqrt{S}\, \tilde{\xi}_h + \sqrt{\frac{n}{J}}\, \tilde{\mu}_h \right) \right)^2 \qquad (5\text{-}16)$$

where $\tilde{\xi}$ and $\tilde{\mu}$ are new random variables with zero mean and unit variance. Since $\tilde{\mu}$ has only J degrees of freedom in offset, a sum of M offsets of $\tilde{\mu}$ can be thought of as a sum of J independent offsets each with a multiplicity of $m = \frac{M}{J}$. Thus, after summing over offset and squaring equation (5-16) becomes

$$NUM = m^2 J^2 S\, \xi'^2 + 2m^2 J\sqrt{nS}\, \xi' \mu' + m^2 n\, \mu'^2 \qquad (5\text{-}17)$$

where μ' and ξ' are new zero mean, unit variance random variables. Since ξ' and μ' are uncorrelated the expected value of the numerator of (5-13), E(NUM) is

$$E(NUM) = m^2 J^2 S + m^2 n = M^2 \left(S + \frac{n}{J^2} \right) \qquad (5\text{-}18)$$

Next we will consider the denominator of (5-13), DEN. Substituting equation (5-14) into equation (5-13) we have

$$DEN = M \sum_{h=1}^{M} \left(\sum_{i=1}^{S} \xi_{ih} + \sum_{k=1}^{n/J} \mu_{kh} \right)^2 \qquad (5\text{-}19)$$

After performing the summations (5-19) becomes

Because we have made several assumptions in getting (5-22) the values in Table 5-1 are only approximate. Noting this we can still make statements about the value of migration in making velocity estimates from random earth data. Since correctly migrated data are independent of offset, their semblance along the true velocity trajectory is unity. Thus, on the basis of Table 5-1 we can conclude that for reasonable data parameters (offset, frequency, travel time, etc.) migration can be expected to increase the semblance along the true velocity trajectory by factors of about 50%.

On the basis of this discussion of Figure 5-12 we can make several general statements about the effects of interference on velocity estimates based on surface recorded random point scatterer earth models. First, the wave fields seen on a section recorded over a random point scatterer earth are primarily controlled by interference effects even when ϕ_{max} is small. Second, interference does not greatly affect velocity estimates if ϕ_{max} is small as in Figures 5-10 and 5-11. Third, velocity estimates based on surface recorded scatterer data are seriously degraded by interference when large amounts of high dip energy (ϕ_{max} not small) are present. Fourth, if ϕ_{max} is large, the accuracy and stability of velocity estimates based on surface recorded data can be improved if ϕ_{max} is reduced by dip filtering prior to velocity estimation. Accuracy and stability can also be improved by limiting the range of offsets used in the estimates to as small an extent as possible. The amount of improvement will depend in detail on the frequency content, the range of dips and the amount of noise present in the data.

$$DEN = mJ\left(mJS\,\xi'^2 + 2m\sqrt{J}\sqrt{\frac{nS}{J}}\;\xi'\,\mu' + mJ\,\frac{n}{J}\,\mu'^2 \right) \qquad (5\text{-}20)$$

Thus, the expected value of the denominator of (5-13) is given by

$$E(DEN) = m^2J^2S + m^2Jn = M^2\left(S + \frac{n}{J}\right) \qquad (5\text{-}21)$$

Substituting equations (5-21) and (5-18) into (5-13) we have

$$\text{Semblance} = \frac{S + \frac{n}{J^2}}{S + \frac{n}{J}} \qquad (5\text{-}22)$$

If we define a ϕ_{max} and a pixel size reasonably consistent with that ϕ_{max} we can count pixels on Figure 5-12 and use (5-22) to estimate semblance. Table 5-1 shows semblance values for three values of ϕ_{max}.

ϕ_{max}	S	n	J	Semblance
15°	14	0	1	1.
30°	14	22	1.5	.8
45°	14	60	3	.6

Table 5-1. Semblance values calculated from Figure 5-12 with equation (5-22).

The discussion of Figure 5-12 has also shown that migration should improve velocity estimates based on random earth data, since, for typical data parameters, it increases the semblance of two-dimensional random earth data along the true velocity hyperbolic by factors of about 50%. (For earth models which are random in three dimensions the semblance increase will be greater). The significance of this increase in semblance can only be determined in the context of a particular noise model. However, the belief is that such semblance increases make velocity estimates based on migrated random earth data significantly less susceptible to the influence of noise than are estimates based on surface random earth data.

A Field Data Example

While Figures 5-5 through 5-11 indicate the usefulness of our migratory approach to velocity estimation when it is applied to synthetic data, the approach must still be tested on field data. By testing the theory of this thesis on samples of field data we hope to establish (1) that for all data examined the method does not degrade velocity estimates, (2) that the method makes needed dip and diffusion corrections to coherent but complex data and (3) that the method makes possible the measurement of velocity from laterally incoherent data. Should we fail in our third objective we have not destroyed the theoretical model. We have merely located regions on the earth where other unidentified factors, perhaps theoretical, perhaps practical, are responsible for the lateral incoherence.

As one portion of test data we shall use some 24-fold data collected near a Gulf Coast diapir. Figure 5-14 shows a stacked section of the test data. We will primarily be interested in the data arriving from the reflectors above the diapir (α in 5-14) and from reflectors interior to the diapir (Ω in 5-14). Hopefully, the discontinuous reflections above the diapir and the sparse arrivals interior to it are the result of a rather discontinuous earth structure which approximates our point scatterer model of a no record area.

Prior to making a 'before and after' comparison of velocity estimates we should briefly discuss the parameters used in downward continuing the test data. The data were migrated using equation (4-23). Thus, each offset was downward continued separately using a constant moveout and migration velocity. The velocity used was 6000 ft/sec. Velocity estimates made from the test data indicate that 'true' velocity increases from about 4800 ft/sec at 0.4 seconds to about 8000 ft/sec at 3.0 seconds. Thus, the early portions of our downward continued data will be over-migrated and the late portions of the data will be undermigrated. Finally, we note that a small amount of dip filtering was used during downward continuation to remove from the data dips which did not meet the gridding and dip restrictions of the downward continuation operator.

Figures 5-15 and 5-16 show short offset sections constructed from the surface and downward continued test data. Figures 5-17, 5-18 and 5-19 depict velocity estimates based on surface and downward continued gathers of the test data. The locations of the gathers used in making these estimates are shown in Figure 5-14. Several common midpoint gathers located at midpoints which bracket the locations of the velocity estimates are shown in Figures 5-20 and 5-21.

There are two aspects in which the difference between surface and migrated estimates is fairly apparent. First, velocity estimates based on the downward continued data are often lower than those based on the surface data. Figure 5-18 which is based on picks made from the data of Figure 5-17 illustrates the lower estimates made from the migrated gathers. This velocity change is most apparent for estimates based on reflections with moderate to steep dip (eg., estimates at times greater than the 1.6 sec in Figure 5-17). The magnitude of these velocity shifts is in reasonable agreement with the velocity changes which can be attributed to the Levin effect.

A second difference between the surface and migrated estimates is that there are often (but not always) fewer 'events' on the migrated estimates than on the surface estimates. Additionally, 'events' are often clustered closer together (in velocity) on the migrated estimates. These differences between the surface and downward continued estimates probably result from a combination of the effect of the dip filtering used during migration, and of the removal of velocity diffusion by the migration process.

Differences between the surface and migrated estimates are most apparent for gathers located in regions of the data where lateral coherence is high (gathers like that shown in 5-17). Where the data coherence is poor (regions labeled α and Ω in Figure 5-14) it is often difficult to distinguish between migrated and unmigrated estimates. Migrated and surface estimates based on data in the α region of 5-14 are often of equally fine quality. Like the synthetic data on the left edge of Figure 5-10, the α region of the test data yields good estimates

in spite of its low coherence. Theoretically, in a random earth we expect diffusion of information from midpoint to adjoining midpoint to reduce the total coherence of the surface data along the best fit hyperbolic of our velocity estimator. Hence, we expect the influence of noise to be greater on the surface estimates. This effect is not apparent, so we might conclude that the α region of the test data is such that the effects of interference or external noise are small. Because the α region of the data looks slightly layered and hence, probably has a small ϕ_{max}, the most likely of these two conclusions is that any interference present in the data does not seriously degrade offset coherence. Both the migrated and surface estimates, based on data interior to the diapir, were fairly noisy. However, there were often fewer events and less spread of events on the migrated estimates than on the surface estimates. The lack of dramatic improvement of estimates after migration may be the result of low signal level or a poor fit of the data to our model.

On the basis of this test example, we can draw several conclusions about the use of downward continuation as a preprocessor for velocity estimation. First, when dip is small and data quality is good, downward continuation appears to have little effect on estimates and hence, does not degrade them. Secondly, when dips are moderate, and data coherence is high, downward continuation makes noticeable shifts in estimated velocities as it removes structurally caused residual moveout from the data. Finally, when the data have poor lateral coherence, migration has only a minor effect on velocity estimates if no significant interference effects are present in the data (eg., ϕ_{max} is small).